æ

A Narrow Range of Transcript-error Rates Across the Tree of Life

Weiyi Li[1], Stephan Baehr[2], Michelle Marasco[3], Lauren Reyes[2], Danielle Brister[2], Craig S. Pikaard[3], Jean-Francois Gout[4], Marc Vermulst[5], and Michael Lynch[2]

[1]Joint Initiative for Metrology in Biology, SLAC National Accelerator Laboratory, Stanford University, Stanford, CA, 94305

[2]Biodesign Center for Mechanisms of Evolution, Arizona State University, Tempe, AZ 85287

[3]Department of Biology, Howard Hughes Medical Institute, Indiana University, Bloomington, IN 47405, USA

[4]Mississippi State University, Department of Biological Sciences, Mississippi State, MS 39762

[5]Leonard Davis School of Gerontology, University of Southern California, Los Angeles, CA, 90089

Email: mlynch11@asu.edu

Abstract. The expression of information encoded in genomes is not error-free. Transcript-error rates are dramatically higher than DNA-level mutation rates, and despite their transient nature, the steady-state load of such errors imposes a burden on cellular performance. However, a broad perspective on the degree to which transcript-error rates are constrained by natural selection and diverge among lineages remains to be developed. Here, we present a genome-wide analysis of transcript-error rates across the Tree of Life, showing that the effects of such errors are most likely at least partially dominant, and possibly synergistic, such that larger cells with more transcripts experience larger error burdens. Despite having a much narrower phylogenetic range of variation than genomic mutation rates, transcript-error rates vary in a manner that is consistent with the drift-barrier hypothesis, previously postulated as an explanatory framework for genome mutation-rate evolution. Thus, the degree to which natural selection is capable of reducing transcript-error rates is a function of both the population-genetic and the cellular environment (effective population size, cell volume, proteome size, and average fitness effects of individual errors). The idea that transcript-error rates are adaptively reduced in genes with high expression finds little support in the data.

Owing to fundamental limitations at the biophysical and biochemical levels, enzymes occasionally engage with inappropriate substrates, leading to permanent errors in the case of genome replication and transient errors in the case of transcriptional and translational products. Like all cellular traits, error rates are subject to natural selection, and are expected to be persistently pushed towards low levels. However, the noise in the evolutionary process associated with random genetic drift inhibits the approach to perfection, as the response to directional selection becomes thwarted once the magnitude of incremental improvement becomes smaller than the magnitude of stochastic evolutionary forces (Ohta 1973; Hartl et al. 1985; Lynch 2007).

No example has yet been found in which natural selection has pushed the performance of a cellular features to the level of refinement dictated by the biophysics barrier, as clearly demonstrable with genome-replication fidelity. In principle, biophysical limits at the molecular level should be independent of the cellular background. Yet, the mutation rate per nucleotide site varies by $\sim 1000\times$ across the Tree of Life, and much of this variation is consistent with patterns of variation in the power of random genetic drift (Lynch et al. 2016; Lynch and Trickovic 2020), with the former scaling negatively with the effective population size and the number of genomic sites under selection. The drift-barrier hypothesis also provides a simple explanation for elevated mutation rates in somatic tissues and for the error-prone nature of DNA polymerases involved in relatively small numbers of nucleotide transactions (Lynch 2008, 2010, 2011; Lynch et al. 2016).

Because they are heritable, errors made at the DNA level can have long-term, cumulative consequences. However, nonheritable cellular errors must also impose a steady-state load on the physiological capacities of cells, even though individual error-containing molecules are transient. Drawing from results on a wide phylogenetic range of species, here we show that transcript-error rates are consistently orders of magnitude greater than genomic mutation rates, and like the latter, scale in a manner consistent with the drift-barrier hypothesis, although with a substantially reduced level of phylogenetic variation.

Results

A phylogenetically diverse set of transcript-error rate estimates. To estimate the incidence of errors per nucleotide site within individual transcripts, we employed the circle-

sequencing method (Lou et al. 2013; Acevedo and Andino 2014), with refinements added to minimize the chance of introduction of additional errors during sample preparation (Gout et al. 2013, 2017; Fritsch et al. 2020; Li and Lynch 2020). Briefly, the method involves isolation, fragmentation, and circularization of cellular RNAs, followed by rolling-circle reverse transcription to produce multiple linked repeats of each fragment. After high-throughput sequencing of the concatenated repeats, the individual reads of each fragment are mutually aligned, enabling the separation of true transcript errors from the substantial sporadic errors introduced into single repeats during reverse transcription and/or DNA sequencing. These methods have been thoroughly validated in a number of ways, including via evaluations of responses to damaged bases, faulty RNA polymerase, and removal of nonsense-mediated decay (Gout et al. 2013, 2017; Fritsch et al. 2020; Chung et al. 2023).

The analyses reported here substantially expand prior work in this area by adding new data for seven bacterial species (*Caulobacter crescentus, Deinococcus radiodurans, Kineococcus radiotolerans, Mycobacterium smegmatis, Pseudomonas fluorescens, Salmonella enterica, Staphylococcus aureus*), one member of the archaea (*Haloferax volcanii*), three unicellular eukaryotes (*Chlamydomonas reinhardtii, Paramecium caudatum, Paramecium tetraurelia*), and a multicellular plant (*Arabidopsis thaliana*). To obtain a broad phylogenetic perspective, in the following comparative analyses, we include prior results for two mammals (human and mouse), the fly (*D. melanogaster*), the nematode (*C. elegans*), budding yeast (*S. cerevisiae*), and four other bacterial species (Gout et al. 2013, 2017; Fritsch et al. 2020; Li and Lynch 2020; Chung et al. 2023). We have not included results from two prior studies (Traverse and Ochman 2016; Reid-Bayliss and Loeb 2017), as these give anomalously high estimates, likely because of the more aggressive methods of mRNA fragmentation used in sample preparation (Gout et al. 2017; Meer et al. 2020).

Three striking patterns are revealed by the data (Figure 1a; Supplemental Table S1). First, transcript-error rates are consistently orders of magnitude higher than genomic mutation rates, with the inflation being $> 10^4\times$ in all unicellular species (except *Mesoplasma florum*), and more on the order of $10^3\times$ for all multicellular eukaryotes, which have elevated DNA-level mutation rates (the latter ratios would be higher if compared to mutation rates per germline subdivision, which are not accurately known but roughly of order 10 in the metazoans in this study). Second, in contrast to the thousand-fold range of variation in the genomic mutation rate among the set of

species evaluated, there is only a three-fold range of variation for transcript-error rates. Third, whereas genomic mutation rates in multicellular eukaryotes are consistently one to two orders of magnitude higher than those in unicellular species, there is no discernible difference in transcript-error rates among major phylogenetic groups. This relative constancy of the transcription-error rate across the Tree of Life is strikingly different from the orders-of-magnitude ranges of variation known for other shared traits, including metabolic rates (DeLong et al. 2010), maximum growth rates (Lynch et al. 2022), and genomic mutation rates (Lynch et al. 2016)

Notably, these elevated rates of transcript error arise despite the capacity of proof-reading in RNA polymerases (Alic et al. 2007; Sydow and Cramer 2009) and despite the presence of multiple mechanisms of surveillance and eradication of certain classes of erroneous mRNAs (e.g., nonsense-mediated decay and nonstop decay; Graille and Séraphin 2012; Kervestin and Jacobson 2012). Nor can these high rates be explained as inadvertent by-products of elevated rates of transcription relative to DNA replication, i.e., as tradeoffs between speed and accuracy. Average speeds of transcript progression exhibit only a small range of phylogenetic variation: 46 bp/sec in *E. coli* (Golding and Cox 2004; Proshkin et al. 2010); 20 to 60 bp/sec in yeasts (Larson et al. 2012; Eser et al. 2016; Lisica et al. 2016; Ucuncuoglu et al. 2016); and 21, 23, and 56 bp/sec in *Drosophila,* rat, and human, respectively (Ardehali and Lis 2009). In contrast, replication rates are typically in the range of 100 to 1000 bp/sec in prokaryotes (Hiriyanna and Ramakrishnan 1986; Stillman 1996; Myllykallio et al. 2000), but just 10 to 50 bp/sec in yeast, flies, and mammals (summarized in Lynch 2007, 2023). Thus, transcription is much slower than replication in bacteria, whereas both processes proceed at comparable rates in eukaryotes. Finally, the transcript-error rate data are inconsistent with the idea that more complex molecular machines are less error prone. The RNA polymerase of eukaryotes contain nearly twice the numbers of subunits per complex as those in prokaryotes (Carter and Drouin 2010), and yet the former gain nothing in terms of transcript fidelity.

Global vs. local control of error rates. It has been suggested previously that in organisms with sufficiently high effective population sizes (i.e., bacteria), selection may be efficient enough to promote features that modulate error rates on a gene-by-gene basis, with such rates being adaptively reduced at genetic loci with the highest levels of expression (Meer et al. 2019). Were this to be true, genome-wide estimates of the error rate would not necessarily be representative

of the true situation at individual nucleotide sites. Aside from the issue of whether the strength of selection on error rates at the single-gene level is ever sufficiently large to enable the evolution of local control, implicit in this argument is the assumption that errors in transcripts are not recessive to their error-free sisters. If this were not the case, lowly-expressed genes would be under stronger selection. Although Meer et al. (2019) found evidence of a weak decline in the C-to-U error rate with increasing expression level in *E. coli* ($\sim$ 2-fold) and C-to-U errors in yeast ($\sim$ 1.2-fold), there was no such pattern for total error rates (merging twelve types of base substitution-errors) in yeast (as previously pointed out in Gout et al. 2017) nor in *E. coli.*

To evaluate this issue more broadly, for each of the 21 species, we divided the range of expression into twenty bins of equal width over the full range of observed expression, and then performed weighted least-squares regressions on the mean expression level. Contrary to Meer et al. (2019), we find a significant positive correlation between error rates and transcription levels in *E. coli* and six other species (and a significant negative correlation for another), although in all cases the overall range of variation across expression level is quite small (Figure 2). Analyzing the data in other ways does not alter this conclusion (Supplementary Table S4).

Might variation in rates of transcription bear on the interpretation of the observed data? As noted above, progression rates of RNA polymerase molecules engaged in transcription are quite similar among diverse organisms. There is, however, variation in the overall rates of transcript production, which is a function of the frequency of RNA polymerase engagement. This can be shown by noting that the steady-state number of transcripts per cell scales across species as $\simeq 6700V^{0.4}$, where V is the cell volume in μm^3 (Lynch and Marinov 2015). Given the average cell volume for a species V, the size at birth is approximately $2V/3$, so a volume equivalent to another $2V/3$ must be produced per cell division. This implies that $\sim 5700(1 + d_tT)V^{0.4}$ transcripts must be produced per cell division, where d_t is the decay rate of transcripts (Supplementary Material), and T is the cell-division time (the term d_tT accounts for transcript turnover within the life of a cell). For an *E. coli*-like cell with $V = 1\,\mu$m^3, a cell-division time of $T = 0.4$ hours under optimal laboratory growth conditions (Lynch et al. 2022), and 4000 genes, the average rate of transcript production is then estimated to be $\sim$ 18 transcripts/gene/hour. On the other hand for budding yeast *S. cerevisiae* with $V \simeq 70\,\mu$m^3, a cell-division time of 3 hours under optimal laboratory growth conditions, and $\sim$ 6000 genes, the average rate of transcript production is $\sim$ 27/gene/hour, and assuming the same decay rate as in *S. cerevisiae,* the fission

yeast *S. pombe* produces an average 32 transcripts/gene/hour. Finally, for a *Paramecium*-like cell with $V \simeq 250,000\,\mu\text{m}^3$, a cell-division time of 10 hours under optimal laboratory growth conditions, and $\sim 25,000$ genes, again assuming the same decay rate as observed in yeast, the average rate of transcript production $\simeq 168$/gene/hour.

These results show that the $\sim$ 10-fold range of variation in transcript production rate is not reflected in phylogenetic differences in transcript-error rates, which is inconsistent with a "wear-and-tear" hypothesis. From these observations on both transcript elongation and overall production rates, we conclude that the transcript-error rate is a general genome-wide process, presumably governed by the features of RNA polymerase complexes and other cellular properties.

One can further infer the difficulties in evolving gene-specific modulation of the transcript-error rate in the following way. The mean number of errors per nucleotide site within a transcript across species is $u \simeq 7 \times 10^{-6}$, so assuming a plausible average effect of a fully expressed mutation on fitness of 0.001 (Lynch 2023), if the error was completely dominant (i.e., there were no masking of the error effects by other transcript copies), the selective advantage of a mutant that completely eliminated errors at the site (e.g., by populating it with an unmutable nucleotide, were such a thing to exist), would be 7×10^{-9}. If the errors were only partially dominant and/or the mutant only partially eliminated the error rate, the selective advantage would be lower (approaching 10^{-9} or smaller). Such a small advantage is beyond the reach of natural selection, given that no known species has $N_e > 10^9$ (Lynch and Trickovic 2020). Thus, although there are small differences in the average rates of transcript-error production in genes with different expression levels in a few species, the most extreme effect ($< 3\times$) is unlikely to be a consequence of selection as opposed to being an inadvertent by-product of other expression-associated processes (Drummond and Wilke 2008).

Evolutionary hypotheses. Taken together, these observations strongly support the idea that the strength and/or efficiency of selection for error-rate reduction is substantially reduced at the level of transcription relative to replication. The lack of patterning in Figure 1a may lead to the impression that there are no explanatory biological factors associated with interspecies variation in the transcript-error rate, and that there is a uniform optimum error rate across the Tree of Life, contrary to the situation with genomic mutation rates (Lynch et al. 2016; McCandlish and Plotkin 2016). However, the error-rate estimates displayed in Figure 1a have standard errors

that are typically $< 10\%$ of the estimates, implying the presence of true parametric differences between species.

One optimization model invokes the high cost of transcription and translation fidelity resulting from the energetic cost of kinetic proofreading (Ehrenberg and Kurland 1984). The idea here is that whereas increasingly accurate transcription and translation is beneficial for cell health, too high a level of accuracy might become offset by the costs of proofreading, which generally consumes ATP/GTP and magnifies the time to progression to successful polymerization (Ehrenberg and Kurland 1984; Kurland and Ehrenberg 1984, 1987). Although such optimizing selection cannot be entirely ruled out, there are three potential issues with this hypothesis. First, it remains unclear whether the theoretical optimum level of transcript accuracy is within the reach of natural selection or beyond the drift barrier. Second, this speed vs. accuracy argument assumes that increases in accuracy can only be achieved via costly proofreading improvement rather than through modifications of the basic accuracy of the pre-proofreading catalytic steps in transcription, which would not necessarily impose any tradeoffs. Finally, the phylogenetic range (or lack thereof) in error rates, in the face of $\sim$ 50-fold differences in cell-division times among study species, remains unexplained.

A radically different optimization hypothesis embraces the too common viewpoint that everything biological must have evolved to maximize organismal fitness, postulating that cellular errors have been wrongly labeled as deleterious (Peltz et al. 1999; Pezo et al. 2004; Bacher et al. 2007; Pan 2013; Ribas de Pouplana et al. 2014; Santos et al. 1999; Wang and Pan 2016). Here, the idea is that organisms "deliberately" make errors in order to expand the chemical diversity of the cell, yielding some variant molecules with large enough fitness-enhancing functions in marginal environments to offset the deleterious effects of other deviants. However, although translational (and presumably transcriptional) inaccuracies can increase during times of stress, on occasion even stochastically creating variants capable of improving a precarious situation, there is no direct evidence that error-prone processes are actively promoted and/or maintained by selection as strategies for adaptively generating variant protein pools, and plenty of evidence to the contrary (Lynch 2023). When cells are stressed, cellular functions go wrong, and there is no obvious reason why transcript-error production should be maintained as a bet-hedging strategy in healthy cells.

Multiple lines of evidence support the idea that the bulk of transcript errors are harmful to

cell fitness. For example, knockouts of the nonsense-mediated decay pathway (which results in the retention of just a small subset of transcription errors) have small but discernible phenotypic effects in the yeasts *S. cerevisiae* and *S. pombe* (Leeds et al. 1992; Dahlseid et al. 1998; Mendell et al. 2000), moderate fitness effects in the nematode *C. elegans* (Hodgkin et al. 1989), and lethal effects in mice (Medghalchi et al. 2001). As many errors in messenger RNAs are manifest in the resultant translational products (which also have longer half lives than their mRNAs), there must be a steady-state error load carried by the many thousands of transcripts contained within individual cells, and this is reflected in proteostatic imbalance in yeast cells with elevated rates of transcription errors (Vermulst et el. 2015). From Lynch and Marinov (2015), the steady-state number of transcripts per cell $\simeq 6700V^{0.4}$, where V is the cell volume in μm^3. Approximating the transcript-error rate as 10^{-5}, assuming an average transcript length of 1 kb, and accounting for transcript decay and replacement per cell lifetime (Supplemental Text), a bacterial cell with $V = 1$ μm^3 is then expected to carry a minimum ~ 350 errors at any point in time. Eukaryotic transcripts are longer, and assuming an average of 2 kb per transcript, a yeast-sized cell with $V \simeq 100$ μm^3 would harbor $\sim 13,600$ errors (or approximately two per gene). A larger ciliate cell with $V \simeq 10^5$ μm^3 would harbor $\sim 10^5$ errors at steady state (approximately four per gene). These numbers are relevant because although individual transcripts typically survive for only a fraction of a cell's lifetime, their protein products can survive for the length of the cell cycle (Supplemental Text).

Given the concerns with models suggesting the adaptive maintenance of high levels of error production by stabilizing selection, we consider an alternative evolutionary model incorporating aspects of the population-genetic and cellular environment that appear most likely to influence the efficiency of selection for transcript-error reduction (Supplementary Text). Under the assumption that selection operates to minimize the incidence of transcript errors, the error-rate for unicellular species is expected to scale inversely with the effective population size (which increases the efficiency of natural selection), the effective proteome size (which increases the target size for error production), and the degree to which the effects of errors are manifest at the level of cellular fitness. The drift barrier, which denotes the lowest level to which selection can reduce the error rate (beyond which the power of drift dominates), is given by

$$u^* \propto \frac{1}{\Delta \cdot N_e \cdot \overline{n}\phi_n \cdot P\overline{L} \cdot \overline{\delta}/k}, \tag{1}$$

where Δ is a measure of the granularity of mutational changes in the error rates of successively improving alleles, i.e., the fractional reduction in the error rate near the drift barrier with the next improving allele; N_e is the effective population size; P is the number of protein-coding genes per genome; $\overline{L}$ is the mean number of codons per gene; $\overline{n}$ is the mean steady-state number of transcripts per cell per gene; $\overline{\delta}$ is the average reduction in fitness per transcript error if fully expressed (i.e., if manifest in all proteins associated with the gene, as in the case of a homozygous genomic mutation); and k is a function of the rates of decay of proteins and transcripts (defined in the Supplementary Text).

The function $\phi_n = \{1 - [x(1-x)C_n^2/2]\}/\overline{n}^x$ is the average dilution factor, with $C_n \simeq 2$ denoting the coefficient of variation in expression level among genes (Supplementary Text). It is a measure of the average degree of expression of a transcript error. When $x = 1$, $\phi_n = 1/\overline{n}$, in which case, the effects of individual errors are additive, and there is no net effect associated with transcript copy numbers, as the product $\overline{n}\phi_n = 1$. For $x < 1$, there is a positive copy-number effect, with $x = 0$ yielding $\phi_n = 1$, implying complete dominance such that $\overline{n}\phi_n$ increases linearly with the number of transcripts per cell; whereas $x < 0$ implies positive synergistic effects. On the other hand, $x > 1$ implies recessivity, with larger numbers of transcripts per gene masking the effects of errors. The parameter $\overline{n}$ can be estimated using the scaling relationship between the mean total transcript numbers/cell and cell volume (Lynch and Marinov 2015; Supplemental Text).

Unfortunately, little information exists for Δ, $\overline{\delta}$, or k, although limited data for bacteria, yeast, and mouse suggest $k = 0.16, 0.32$, and 0.38, respectively (Supplementary Text). Ignoring these factors will lead to noise in downstream analyses, but logarithmic transformation allows a consideration of the transcript-error rate with respect to the composite quantity $N_e \cdot \overline{n}\phi_n \cdot P\overline{L}$, which is equivalent to the product of the effective population size and the effective number of errors per cell. The optimal fit to the data for unicellular species corresponds to $x \simeq 1.0$ (Figure 1b), i.e., additivity of the effects of transcript errors. However, although the optimal fit is moderately good ($r^2 = 0.33$, P < 0.015, df $= 14$), the support interval for x ranges from -4.5 (strongly synergistic) to 2.5 (moderately recessive), with more support in the direction of synergism.

Although statistically significant, the slope of the optimized regression, -0.095 (SE $=$ 0.038), is far smaller than the expectation of -1.0 if the composite parameter alone governed

the evolution of the error rate. (With extreme support values of $x = -4.5$ and 2.5 the best fit slopes are -0.020 and -0.079, respectively). This relatively shallow level of scaling may be a consequence of two effects. First, because a regression coefficient is equal to the ratio of the covariance and the variance of the explanatory variable, whenever there is sampling variance in the latter, the regression estimate will be biased towards zero. All of the components of $N_e \cdot \overline{n}\phi_n \cdot P\overline{L}$ are subject to unknown levels of sampling error, but in the extreme case in which the overall variance of the composite quantity is inflated two-fold by sampling error, a more unbiased regression estimate would be $\sim -0.095 \times 2 = -0.19$. Second, to alter the slope involving the full set of terms in Equation 1 to a value near -1, the composite quantity $(\Delta\overline{\delta}/k)$ needs to decline by a factor of 5 to 10 in coordination with an increase of $N_eP\overline{L}$ across the full range of data in Figure 1. This seems plausible. As noted above, the limited available data suggest that k approximately doubles in size from small bacteria to larger eukaryotic cells. In addition, Δ is expected to decline with increasing $N_eP\overline{L}$, owing to the fact that as the error rate declines, there is less room for further improvement. Least clear is whether the average effects of mutations $(\overline{\delta})$ decrease with increasing $N_eP\overline{L}$. However, such a pattern is expected from the standpoint of bioenergetic considerations (Lynch and Marinov 2015), as individual mutations imposing a bioenergetic cost must be weighed against the total energy budget of a cell, which increases isometrically with cell volume.

There are at least two reasons why the expectations of the unicellular model described above may not strictly apply to multicellular species. First, cell sizes can vary substantially among tissue types, and if fitness defects associated with errors are correlated with cell size, the use of an average cell volume to estimate the relevant mean number of transcripts per cell will be problematical. Second, there are potential higher-order effects of errors associated with multicellularity, including defects in cell adhesion, cell migration, and development, which may operate in synergistic ways that would magnify the level of selection to reduce the transcript-error rate. Nonetheless, as can be seen in Figure 1b, the error-rate estimates for multicellular species are similar to the model expectation, with the exception of the relatively low rate for human, although all values are below the regression line for unicellular species.

Finally, the focus of the preceding analyses has been on the production of errors within nuclear messenger RNAs. Prokaryotes deploy just a single RNA polymerase in all transcription, but in eukaryotes, one complex (Pol II) is reserved for the production of nuclear messenger

RNAs and micro RNAs, another (Pol I) for the synthesis of the ribosomal RNA subunits, a third (Pol III) for transfer-RNA and 5S-rRNA production, and still another for transcription in the mitochondrion (Werner and Grohmann 2011; Basu et al. 2020). For yeast and human-cell analyses, sufficient data exist to compare the fidelities of the four complexes. In yeast, Pols I and II have similar error rates, $4.3(SE = 0.04)$ and $3.6(0.03) \times 10^{-6}$, respectively, whereas the rates for mt Pol and Pol III are inflated by factors of two to four, $9.3(1.5)$ and $17.0(1.7) \times 10^{-6}$, respectively (Gout et al. 2017; Fritsch et al. 2021). Likewise, in human cells, the error rates of Pols I and II are nearly identical, $4.1(0.03)$ and $4.2(0.02) \times 10^{-6}$, respectively, whereas the rates for mt Pol and Pol III are inflated by factors of two to three, $10.0(0.1)$ and $13.0(1.0) \times 10^{-6}$, respectively (Chung et al. 2022). For the *Arabidopsis* results reported here, there are only sufficient data for estimates of the error rates of Pol II and mt Pol, $7.3(0.5) \times 10^{-6}$ and $3.3(0.3) \times 10^{-5}$, respectively. These observations are qualitatively consistent with the drift-barrier hypothesis in that the mutational target sizes for mt Pol and Pol III are substantially reduced relative to that for Pol II, whereas errors in ribosomal RNAs may have cascading effects on the quality of all downstream translational products.

Conclusions

In summary, across the Tree of Life, natural selection is consistently incapable of reducing the rate of production of errors in mRNAs to the level of mutation at the DNA level, despite the fact that the polymerases involved in both kinds of activity are endowed with proof-reading capacity and engage with the same substrate molecule. Nonetheless, as in the case of mutation rates at the genomic level, transcript-error rates vary among species in a manner that is consistent with the expectations of the drift-barrier hypothesis, which postulates that the ability of selection to reduce the rate of error production is positively correlated with the sizes of the relevant mutational targets and with the influence of the effective population size on the power of random genetic drift. Further work is needed to explain why the transcript-error rate is specifically constrained to a range of 3 to 20 $\times 10^{-6}$, making it perhaps the most phylogenetically invariant character observed across the prokaryotic and eukaryotic domains.

The consistently high rates of transcript-error production across diverse lineages do not appear to be a physical by-product of high transcriptional activity. Rather, the small but sig-

nificant phylogenetic variance in rates appears to be a consequence of variation in the combined effects of population-genetic and cellular environments, with the overall negative consequences of transcript errors being small enough for selection for further improvement to be stalled at the drift barrier. Although general patterns may not be noticeable within narrow phylogenetic lineages, taken across the entire Tree of Life, it appears that the efficiency of natural selection varies to a significant enough level to influence a diversity of cellular features (Lynch et al. 2016, 2022).

Methods

Prokaryote strains, culture media and growth conditions. All prokaryotes were initiated from single colonies and grown in liquid culture to mid-exponential growth phase upon harvest. Details are listed in Supplementary Table S2.

Single-celled eukaryotes. *Paramecium* strains were inherited from the lab of John Preer at Indiana University. Strain s-51 (WT *P. tetraurelia*) and strain 43c3d (WT *P. caudatum*) were maintained in wheat-grass medium inoculated with *Klebsiella* bacteria and grown at room temperature, $\sim 23°$C. *Paramecium* were diluted and single cell isolates were obtained, initially growing one cell in 250 μL, then expanding to 500 μL, and then 1 mL in consecutive days, as cell divisions occurred. This doubling continued daily until final volumes of ~ 5 liters were reached. 4.5 liters of *Paramecium* were then cleaned with four layers of cheesecloth laid inside a funnel, such that large debris was collected by the cheesecloth, and *Paramecium* and bacteria passed through. Next, the *Paramecium* were retained with a 15-μm cloth bottomed sifting drum, through which bacteria passed. Finally, the *Paramecium* were washed and concentrated with Dryls buffer, and picked up with a plastic wide-bore Pasteur pipette, and collected in 15-mL tubes. Th latter were then spun for 8 minutes at 4000 RCF to obtain a stable pellet. After removing supernatant, the cells were resuspended following the directions of the RNEASY Midi Kit (Qiagen), and total RNA was extracted following manufacturer specifications.

Strain CC-503 cw92 mt+ of *Chlamydomonas reinhardtii,* obtained from the *Chlamydomonas* Stock Center, was grown in YA media at 20°C on a 16 hr light:8 hr cycle of ~ 120 μmol M^{-2} sec^{-1}, shaken at 40 rpm. Cells were streaked on YA plates, and single colonies were picked and

placed into 50-mL tubes of YA. Cells were then grown to O.D. ~ 0.6, and harvested from liquid suspension, avoiding pelleted cells sitting at the bottom of the tube. The 49 mL of suspended cells were transferred to a new tube and spun for 1 minute at 7500 RCF. The pellet was then resuspended in 750 μL of CTAB lysis buffer, and split three ways into 1.5 mL tubes, roughly 250 μL per tube. RNA extraction was performed, with special care taken to lyse cell walls, using a tissue grinder in a douncing pattern to lyse the cells for 3 minutes, with breaks to disperse foaming. 150 μL of 3 M sodium acetate was added to the lysate, vortexed for 10 seconds, followed by 1 mL of 100% ETOH, and vortexed again. After a 3-minute incubation on ice, the split samples were then recombined in a 15-mL tube, and spun at 7500x G for 15 minutes. The supernatant was removed, and the pellet resuspended in the contents of the Qiagen RNEASY midi kit. Total RNA was obtained and used according to the general RNA-rolling-circle protocol, as described in Gout et al. (2017).

Plant materials. Leaf tissues of 2-week-old *Arabidopsis thaliana* Col-0 plants were ground in liquid nitrogen to a powder, and total RNA was extracted using TRIzol (ThermoFisher Scientific). rRNA was depleted by the Ribo-Zero rRNA Removal Kit (Plant Leaf) (Illumina) to enrich mRNAs for subsequent library preparations.

Sequencing library construction. Three to four biological replicates were prepared for each species. The total RNA extraction, rRNA depletion, and construction of rolling circle sequencing library were done as previously described (Gout et al. 2017; Fritsch et al. 2020; Li and Lynch 2020). To evaluate whether circularization of RNAs during sequencing library preparations introduce bias in RNA abundances, we also prepared regular RNA sequencing libraries for *D. radiodurans, P. fluorescens, S. enterica,* and *S. aureus.* Total RNAs of these four species were split into two halves, one to construct modified CirSeq libraries and the other for regular mRNA-seq libraries. Illumina SE300 and SE100 reads were generated for CirSeq and regular RNA-seq libraries, respectively.

Data analysis. Transcript errors were called following the analysis pipeline as previously described (Gout et al. 2017; Fritsch et al. 2020; Li and Lynch 2020) with some modifications.Different from the case of genetic mutations where all derived reads tend to show mis-

matches from the reference, transcript errors result in mismatches of reads at a low frequency. A statistical framework proposed in Meer et al 2020 was followed to accurately call transcript errors according to the frequency of transcript errors at individual nucleotide loci. Transcript errors were initially called if consensus base calls mismatch with the reference and the consensus-read coverage of the corresponding nucleotide locus was ≥ 50. A transcriptome-wide transcript-error rate was estimated accordingly after every nucleotide locus was surveyed. Assuming the number of transcript errors at each nucleotide locus follows a binomial distribution, the expected number of transcript errors at each locus was calculated according to the consensus-read coverage of the corresponding locus and the current estimate of the transcriptome-wide transcript-error rate. Outlier loci where the observed number of transcript errors was significantly larger than the expected one (Bonferroni-corrected P values of 0.05), were excluded and an updated estimate of the transcriptome-wide transcript-error rate was obtained. In the next round of iteration, revised expectations on the number of transcript errors observed from each locus were formulated by the updated estimate of transcript-error rate, outliers loci were excluded, and the estimate of the transcript-error rate was further updated. The final estimate of the transcriptome-wide transcript-error rate was obtained after convergence.

To evaluate gene expression levels, the Tophat-Cufflink pipeline was followed to calculate fpkm of each gene. To evaluate whether bias on the estimation of RNA abundances were introduced by circularization, only CirSeq reads that contain tandem repeats were used for the expression level analysis.

Estimates of effective population sizes. The effective population sizes (N_e) of prokaryotes in this study (not previously reported) were estimated from measures of silent-site heterozygosity in protein-coding genes (π_s), which has an expectation of $2N_e\mu_g$, where μ_g denotes the base-substitution rate per nucleotide per generation, available from previous mutation-accumulation studies (Supplementary Table 1). π_s was estimated from nucleotide heterozygosity of four-fold degenerative sites across the whole genome from data deposited at NCBI (Supplementary Table S3).

Data availability Sequencing data for prokaryotes, *A. thaliana*, *C. reinhardtii*, *P. caudatum*, and *P. tetraurelia* are deposited in NCBI with the BioProject Number PRJNA778257, PR-

JNA791609, PRJNA847594, PRJNA844889, and PRJNA839092, respectively.

Code availability Source code for analysis is available at https://github.com/LynchLab / CirSeq4TranscriptErrors.

Acknowledgments

This research was supported by the Multidisciplinary University Research Initiative awards W911NF-09-1-0444 and W911NF-09-1-0444 from the US Army Research Office, National Institutes of Health award R35-GM122566-01, National Science Foundation award DBI-2119963, and Grant 735927 from the Moore-Simons Project on the Origin of the Eukaryotic Cell to ML, National Institutes of Health award GM077590 and Howard Hughes Medical Institute Investigator funds to CSP, and National Institutes of Aging award R01-AG054641-01 to MV.

References

Acevedo, A., and R. Andino. 2014. Library preparation for highly accurate population sequencing of RNA viruses. Nature Protocols 9: 1760-1769.

Alic, N., N. Ayoub, E. Landrieux, E. Favry, P. Baudouin-Cornu, M. Riva, and C. Carles. 2007. Selectivity and proofreading both contribute significantly to the fidelity of RNA polymerase III transcription. Proc. Natl. Acad. Sci. USA 104: 10400-10405.

Ardehali, M. B., and J. T. Lis. 2009. Tracking rates of transcription and splicing *in vivo.* Nat. Struct. Mol. Biol. 16: 1123-1124.

Bacher, J. M., W. F. Waas, D. Metzgar, V. de Crécy-Lagard, and P. Schimmel. 2007. Genetic code ambiguity confers a selective advantage on *Acinetobacter baylyi.* J. Bacteriol. 189: 6494-6496.

Basu, U., A. M. Bostwick, K. Das, K. E. Dittenhafer-Reed, and S. S. Patel. 2020. Structure, mechanism, and regulation of mitochondrial DNA transcription initiation. J. Biol. Chem. 295: 18406-18425.

Carter, R., and G. Drouin. 2010. The increase in the number of subunits in eukaryotic RNA polymerase III relative to RNA polymerase II is due to the permanent recruitment of general transcription factors. Mol. Biol. Evol. 27: 1035-1043.

Chung, C. B. M. Verheijen, X. Zhang, B. Huang, A. Coakley, E. McGann, E. Wade, O. Dinep-Schneider, J. LaGosh, M. Anagnostou, S. Simpson, K. Thomas, J. M. Ernst, A. Rattray, M. Lynch, M. Kashlev, B. A. Benayoun, Z. Li, J. Strathern, J.-F. Gout, and M. Vermulst. 2023. The fidelity of transcription in human cells. Proc. Natl. Acad. Sci. USA 120: e2210038120.

Dahlseid, J. N., J. Puziss, R. L. Shirley, A. L. Atkin, P. Hieter, and M. R. Culbertson. 1998. Accumulation of mRNA coding for the ctf13p kinetochore subunit of *Saccharomyces cerevisiae* depends on the same factors that promote rapid decay of nonsense mRNAs. Genetics 150: 1019-1035.

DeLong, J. P., J. G. Okie, M. E. Moses, R. M. Sibly, and J. H. Brown. 2010. Shifts in metabolic scaling, production, and efficiency across major evolutionary transitions of life. Proc. Natl. Acad. Sci. USA 107: 12941-12945.

Drummond, D. A., and C. O. Wilke. 2008. Mistranslation-induced protein misfolding as a

dominant constraint on coding-sequence evolution. Cell 134: 341-352.

Ehrenberg, M., and C. G. Kurland. 1984. Costs of accuracy determined by a maximal growth rate constraint. Quart. Rev. Biophys. 17: 45-82.

Eser, P., L. Wachutka, K. C. Maier, C. Demel, M. Boroni, S. Iyer, P. Cramer, and J. Gagneur. 2016. Determinants of RNA metabolism in the *Schizosaccharomyces pombe* genome. Mol. Syst. Biol. 12: 857.

Fritsch, C., J.-F. Gout, S. Haroon, A. Towheed, X. Zhang, Y. Song, S. Simpson, D. Wallace, K. Thomas, M. Lynch, and M. Vermulst. 2020. Genome-wide surveillance of transcription errors in response to genotoxic stress. Proc. Natl. Acad. Sci. USA 118: e2004077118.

Golding, I., and E. C. Cox. 2004. RNA dynamics in live *Escherichia coli* cells. Proc. Natl. Acad. Sci. USA 101: 11310-11305.

Gout, J. F., W. Li, C. Fritsch, A. Li, S. Haroon, L. Singh, D. Hua, H. Fazelinia, Z. Smith, S. Seeholzer, et al. 2017. The landscape of transcription errors in eukaryotic cells. Sci. Adv. 3: e1701484.

Gout, J. F., W. K. Thomas, Z. Smith, K. Okamoto, and M. Lynch. 2013. Large-scale detection of *in vivo* transcription errors. Proc. Natl. Acad. Sci. USA 110: 18584-18589.

Graille, M., and B. Séraphin. 2012. Surveillance pathways rescuing eukaryotic ribosomes lost in translation. Nat. Rev. Mol. Cell Biol. 13: 727-735.

Hartl, D. L., D. E. Dykhuizen, and A. M. Dean. 1985. Limits of adaptation: the evolution of selective neutrality. Genetics 111: 655-674.

Hiriyanna, K. T., and T. Ramakrishnan. 1986. Deoxyribonucleic acid replication time in *Mycobacterium tuberculosis* H37 Rv. Arch. Microbiol. 144: 105-109.

Hodgkin, J., A. Papp, R. Pulak, V. Ambros, and P. Anderson. 1989. A new kind of informational suppression in the nematode *Caenorhabditis elegans*. Genetics 123: 301-313.

Kervestin, S., and A. Jacobson. 2012. NMD: a multifaceted response to premature translational termination. Nat. Rev. Mol. Cell Biol. 13: 700-712.

Kurland, C. G., and M. Ehrenberg. 1984. Optimization of translation accuracy. Prog. Nucleic Acid Res. Mol. Biol. 31: 191-219.

Kurland, C. G., and M. Ehrenberg. 1987. Growth-optimizing accuracy of gene expression. Annu. Rev. Biophys. Biophys. Chem. 16: 291-317.

Larson, M. H., J. Zhou, C. D. Kaplan, M. Palangat, R. D. Kornberg, R. Landick, and S. M. Block. 2012. Trigger loop dynamics mediate the balance between the transcriptional fidelity and speed of RNA polymerase II. Proc. Natl. Acad. Sci. USA 109: 6555-6560.

Leeds, P., J. M. Wood, B. S. Lee, and M. R. Culbertson. 1992. Gene products that promote mRNA turnover in *Saccharomyces cerevisiae.* Mol. Cell. Biol. 12: 2165-2177.

Li, W., and M. Lynch. 2020. Universally high transcript error rates in bacteria. eLife 9: e54898.

Lisica, A., C. Engel, M. Jahnel, É. Roldán, E. A. Galburt, P. Cramer, and S. W. Grill. 2016. Mechanisms of backtrack recovery by RNA polymerases I and II. Proc. Natl. Acad. Sci. USA 113: 2946-2951.

Long, H., W. Sung, S. Kucukyildirim, E. Williams, W. Guo, C. Patterson, C. Gregory, C. Strauss, C. Stone, C. Berne, et al. 2017. Evolutionary determinants of genome-wide nucleotide composition. Nature Ecol. Evol. 2: 237-240.

Lou, D. I., J. A. Hussmann, R. M. McBee, A. Acevedo, R. Andino, W. H. Press, and S. L. Sawyer. 2013. High-throughput DNA sequencing errors are reduced by orders of magnitude using circle sequencing. Proc. Natl. Acad. Sci. USA 110: 19872-19877.

Lynch, M. 2007. The Origins of Genome Architecture. Sinauer Assocs., Inc., Sunderland, MA.

Lynch, M. 2008. The cellular, developmental, and population-genetic determinants of mutation-rate evolution. Genetics 180: 933-943.

Lynch, M. 2010. Evolution of the mutation rate. Trends Genetics 26: 345-352.

Lynch, M. 2011. The lower bound to the evolution of mutation rates. Genome Biol. Evol. 3: 1107-1118.

Lynch, M. 2023. Evolutionary Cell Biology: The Origins of Cellular Architecture. Oxford Univ. Press, Oxford, UK (in prep.; online copies of all chapters at cellularevolution.asu.edu).

Lynch, M., M. Ackerman, J.-F. Gout, H. Long, W. Sung, W. K. Thomas, and P. L. Foster. 2016. Genetic drift, selection, and evolution of the mutation rate. Nature Rev. Genetics 17: 704-714.

Lynch, M., and G. K. Marinov. 2015. The bioenergetic costs of a gene. Proc. Natl. Acad. Sci. USA 112: 15690-15695.

Lynch, M., and B. Trickovic. 2020. A theoretical framework for evolutionary cell biology. J. Mol. Biol. 432: 1861-1879.

Lynch, M., B. Trickovic, and C. P. Kempes. 2022. Evolutionary scaling of maximum growth rates with organism size. Scientific Reports (in revision).

McCandlish, D. M., and J. B. Plotkin. 2016. Transcriptional errors and the drift barrier. Proc. Natl. Acad. Sci. USA 113: 3136-3138.

Medghalchi, S. M., P. A. Frischmeyer, J. T. Mendell, A. G. Kelly, A. M. Lawler, and H. C. Dietz. 2001. Rent1, a trans-effector of nonsense-mediated mRNA decay, is essential for mammalian embryonic viability. Hum. Mol. Genet. 10: 99-105.

Meer, K. M., P. G. Nelson, K. Xiong, and J. Masel. 2020. High transcriptional error rates vary as a function of gene expression level. Genome Biol. Evol. 12: 3754-3761.

Mendell, J. T., S. M. Medghalchi, R. G. Lake, E. N. Noensie, and H. C. Dietz. 2000. Novel Upf2p orthologues suggest a functional link between translation initiation and nonsense surveillance complexes. Mol. Cell. Biol. 20: 8944-8957.

Myllykallio, H., P. Lopez, P. López-García, R. Heilig, W. Saurin, Y. Zivanovic, H. Philippe, and P. Forterre. 2000. Bacterial mode of replication with eukaryotic-like machinery in a hyperthermophilic archaeon. Science 288: 2212-2215.

Ohta, T. 1973. Slightly deleterious mutant substitutions in evolution. Nature 246: 96-98.

Pan, T. 2013. Adaptive translation as a mechanism of stress response and adaptation. Annu. Rev. Genet. 47: 121-137.

Peltz, S. W., A. B. Hammell, Y. Cui, J. Yasenchak, L. Puljanowski, and J. D. Dinman. 1999. Ribosomal protein L3 mutants alter translational fidelity and promote rapid loss of the yeast killer virus. Mol. Cell Biol. 19: 384-391.

Pezo, V., D. Metzgar, T. L. Hendrickson, W. F. Waas, S. Hazebrouck, V. Döring, P. Marlière, P. Schimmel, and V. De Crècy-Lagard. 2004. Artificially ambiguous genetic code confers growth yield advantage. Proc. Natl. Acad. Sci. USA 101: 8593-8597.

Proshkin, S., A. R. Rahmouni, A. Mironov, and E. Nudler. 2010. Cooperation between translating ribosomes and RNA polymerase in transcription elongation. Science 328: 504-508.

Reid-Bayliss, K. S., and L. A. Loeb. 2017. Accurate RNA consensus sequencing for high-fidelity detection of transcriptional mutagenesis-induced epimutations. Proc. Natl. Acad. Sci. USA 114: 9415-9420.

Ribas de Pouplana, L., M. A. Santos, J. H. Zhu, P. J. Farabaugh, and B. Javid. 2014. Protein mistranslation: friend or foe? Trends Biochem. Sci. 39: 355-362.

Santos, M. A., C. Cheesman, V. Costa, P. Moradas-Ferreira, and M. F. Tuite. 1999. Selective advantages created by codon ambiguity allowed for the evolution of an alternative genetic code in *Candida* spp. Mol. Microbiol. 31: 937-947.

Stillman, B. 1996. Cell cycle control of DNA replication. Science 274: 1659-1664.

Sydow, J. F., and P. Cramer. 2009. RNA polymerase fidelity and transcriptional proofreading. Curr. Opin. Struct. Biol. 19: 732-739.

Traverse, C. C., and H. Ochman. 2016. Conserved rates and patterns of transcription errors across bacterial growth states and lifestyles. Proc. Natl. Acad. Sci. USA 113: 3311-3316.

Ucuncuoglu, S., K. L. Engel, P. K. Purohit, D. D. Dunlap, and D. A. Schneider, and L. Finzi. 2016. Direct characterization of transcription elongation by RNA polymerase I. PLoS One 11: e0159527.

Vermulst, M., A. S. Denney, M. J. Lang, C.-W. Hung, S. M., M. A. Moseley, J. W. Thompson, V. Madden, J. Gauer, K. J. Wolfe, D. W. Summers, J. Schleit, G. L. Sutphin, S. Haroon, A. Holczbauer, J. Caine, J. Jorgenson, D. Cyr, M. Kaeberlein, J. N. Strathern, M. C. Duncan. and D. A. Erie. 2015. Transcription errors induce proteotoxic stress and shorten cellular lifespan. Nature Comm. 6: 8065.

Wang, X., and T. Pan. 2016. Stress response and adaptation mediated by amino acid misincorporation during protein synthesis. Adv. Nutr. 7: 773S-779S.

Werner, F., and D. Grohmann. 2011. Evolution of multisubunit RNA polymerases in the three domains of life. Nat. Rev. Microbiol. 9: 85-98.

Figure 1a) Transcript-error and genomic-mutation rates (substitutions per nucleotide site) for species across the Tree of Life. Genomic-mutation rate data are derived from Lynch et al. (2016), Long et al. (2017), and Lynch and Trickovic (2020). Diagonal dashed lines are isoclines for ratios of the two rates. **1b)** Regression fit of the observed transcript-error rates for unicellular species to the composite parameter described in the text; the best fit (given by the regression line) is obtained with exponent value $x = 1.0$ (with the gradient of the fits with alternative x values given in the inset, and the support interval within which the regression remains significant at the 0.05 level denoted by the solid points). The data points for multicellular eukaryotes are given for reference, but not used in the regression. PL denotes the total proteome size (summed over all codons, in megabases). Standard errors of the individual measures of transcript-error rates are generally smaller than the widths of the points. All data, including those for unlabeled bacteria, are contained in Supplementary Table S1. *At = Arabidopsis thaliana; Ce = Caenorhabditis elegans; Cr = Chlamydomonas reinhardtii; Dm = Drosophila melanogaster; Hs = Homo sapiens; Mf = Mesoplasma florum; Mm = Mus musculus; Pc = Paramecium caudatum; Pt = Paramecium tetraurelia; Sc = Saccharomyces cerevisiae.*

Figure 2. Transcript-error rates of protein-coding genes at different expression levels. Protein-coding genes were grouped into 20 bins according to ranks of expression levels, from the bottom 5 percentile to the top 5 percentile, to ensure an equal number of genes in each bin. Expression levels of genes (FPKM) were obtained from CirSeq reads, which provide estimates for expression levels consistent with regular RNA-seq reads (Figure S1). Error rates of bins are the mean transcript-error rates of all genes in the corresponding bins; error bars indicate standard errors of the mean error rates. Weighted least-square linear regression analyses were carried out on the mean transcript-error rates and log-transformed expression levels of 20 bins. Weights are $(1/SE)^2$, where SE is the standard error of the bin mean. Yellow dashed lines represent weighted least-squares regressions, with 95% confidence intervals indicated in gray; gray dots indicate bins with weights equal to 0, which cannot be included in the logarithmic regressions, but their lack of inclusion in the weighted analyses biases the positive regressions in a downward fashion. In the individual-gene analyses (Supplemental Table S4), genes with 0 error rates were included. Regressions with P-values less than 0.05/21 (Bonferroni correction for regression analyses for 21 species) are considered statistically significant.

Figure 1

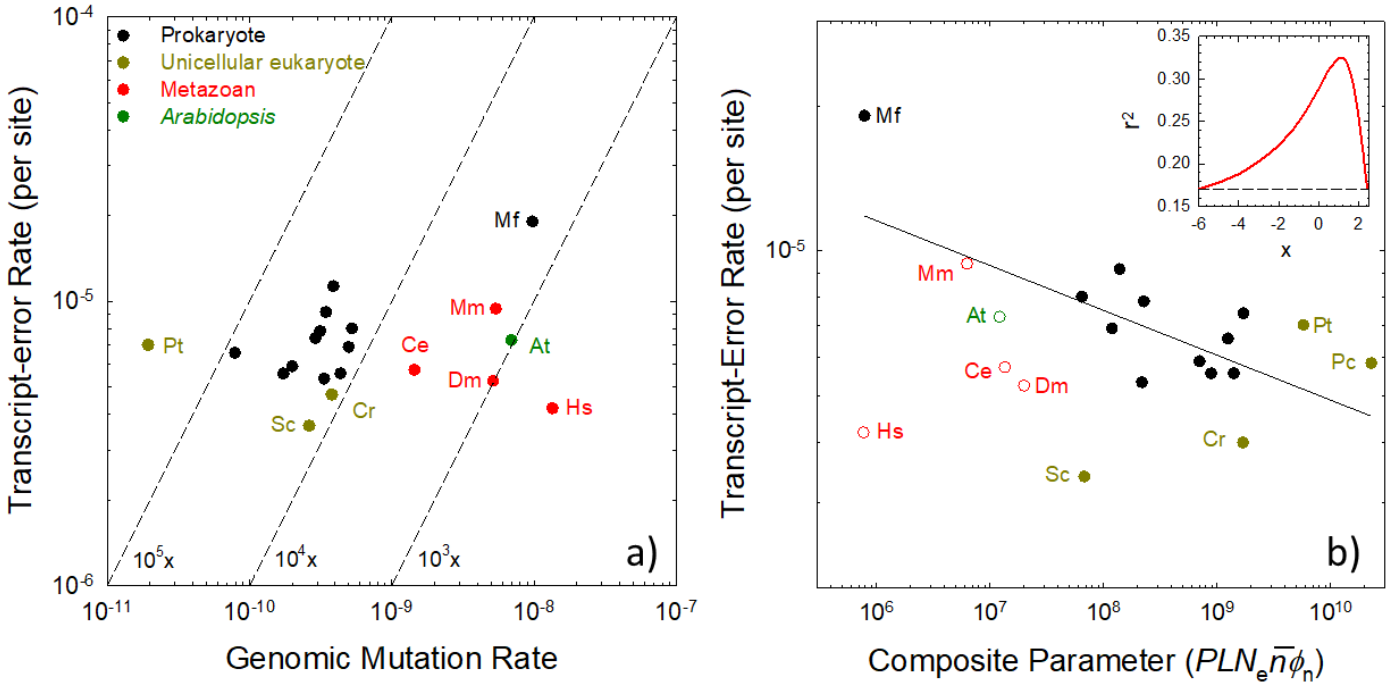
Prokaryote
Unicellular eukaryote
Metazoan
Arabidopsis
Transcript-error Rate (per site)
Genomic Mutation Rate
Mf
Mm
Ce
At
Dm
Hs
Pt
Sc
Cr
10^5x
10^4x
10^3x
a)
Transcript-Error Rate (per site)
Composite Parameter (PLN_e n̄ φ_n)
r^2
x
Pc
b)

Figure 2

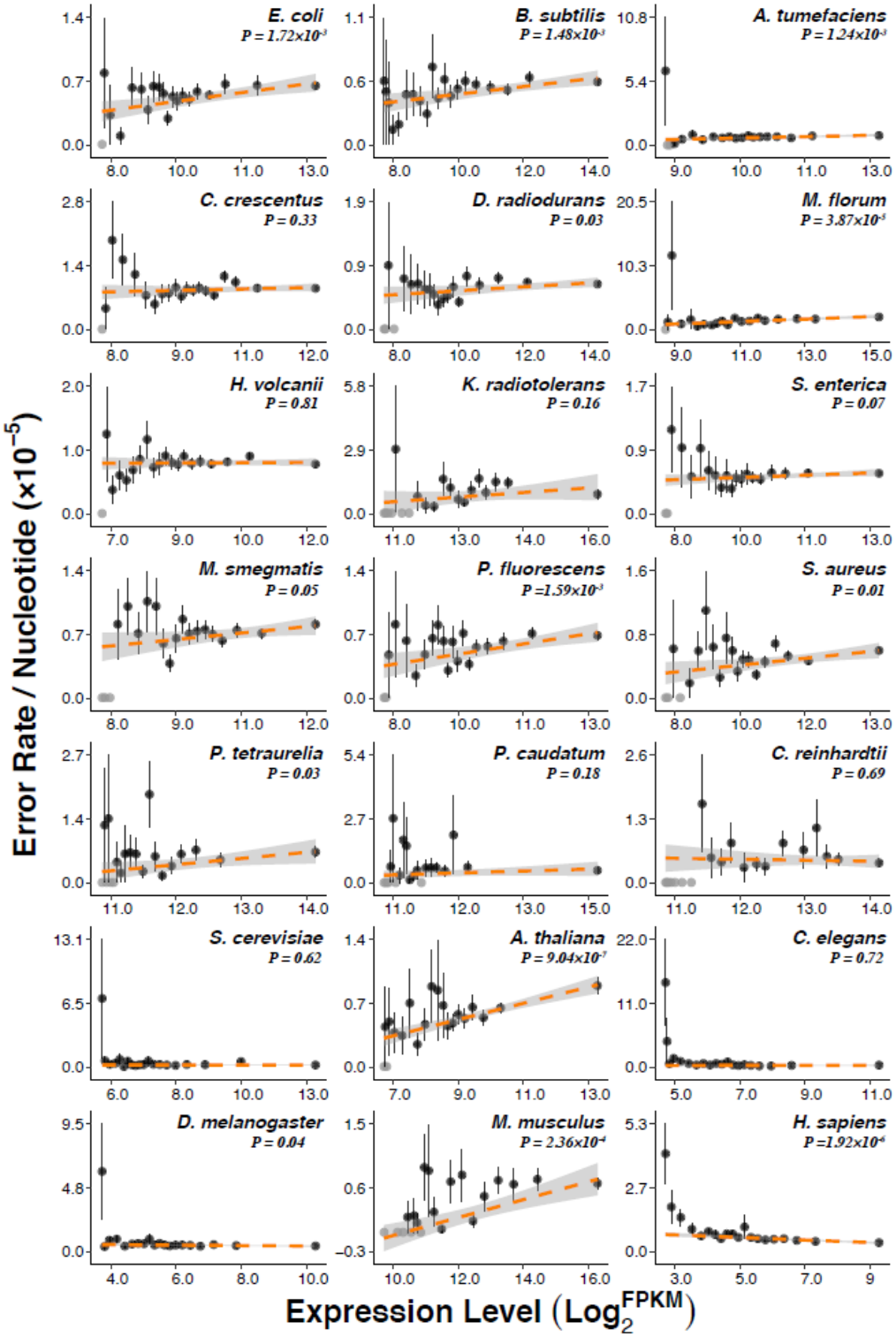
E. coli
P = 1.72×10-3
B. subtilis
P = 1.48×10-3
A. tumefaciens
P = 1.24×10-3
C. crescentus
P = 0.33
D. radiodurans
P = 0.03
M. florum
P = 3.87×10-3
H. volcanii
P = 0.81
K. radiotolerans
P = 0.16
S. enterica
P = 0.07
M. smegmatis
P = 0.05
P. fluorescens
P =1.59×10-3
S. aureus
P = 0.01
P. tetraurelia
P = 0.03
P. caudatum
P = 0.18
C. reinhardtii
P = 0.69
S. cerevisiae
P = 0.62
A. thaliana
P = 9.04×10-7
C. elegans
P = 0.72
D. melanogaster
P = 0.04
M. musculus
P = 2.36×10-4
H. sapiens
P =1.92×10-4
Error Rate / Nucleotide (×10−5)
Expression Level (Log2FPKM)